

The ionospheric eclipse factor method (IEFM) and its application to determining the ionospheric delay for GPS

Y. Yuan · C. C. Tscherning · P. Knudsen ·
G. Xu · J. Ou

Received: 15 February 2006 / Accepted: 15 March 2007 / Published online: 12 April 2007
© Springer-Verlag 2007

Abstract A new method for modeling the ionospheric delay using global positioning system (GPS) data is proposed, called the ionospheric eclipse factor method (IEFM). It is based on establishing a concept referred to as the ionospheric eclipse factor (IEF) λ of the ionospheric pierce point (IPP) and the IEF's influence factor (IFF) $\bar{\lambda}$. The IEF can be used to make a relatively precise distinction between ionospheric daytime and nighttime, whereas the IFF is advantageous for describing the IEF's variations with day, month, season and year, associated with seasonal variations of total electron content (TEC) of the ionosphere. By combining λ and $\bar{\lambda}$ with the local time t of IPP, the IEFM has the ability to precisely distinguish between ionospheric daytime and nighttime, as well as efficiently combine them during different seasons or months over a year at the IPP. The IEFM-based ionospheric delay estimates are validated by combining an absolute positioning mode with several ionospheric delay

correction models or algorithms, using GPS data at an international Global Navigation Satellite System (GNSS) service (IGS) station (WTZR). Our results indicate that the IEFM may further improve ionospheric delay modeling using GPS data.

Keywords GPS ionospheric delay correction algorithm · Ionospheric eclipse factor (IEF) · Ionospheric eclipse factor method (IEFM) · Network real-time-kinematic (RTK)

1 Introduction

After the discontinuation of Selective Available (SA) on 1 May 2000, the ionosphere became the dominant error source in GPS navigation and positioning. In return, GPS has now become an important technique for ionosphere research using both code pseudorange and carrier-phase measurements through extracting precise total electron content (TEC) information (e.g., Coster et al. 2003).

As an approximation, the ionosphere may be considered as a thin layer, i.e., an ionospheric spherical shell, at a height of H_{ipp} . The ionospheric pierce point (IPP) is the intersection point of the line of sight between the receiver and the GPS satellite with the quasi-shell of the ionosphere above the Earth's surface. This assumption is usually adopted in GPS ionosphere research, and was also proposed by the international GNSS service (IGS) ionosphere working group (Feltens and Schaer 1998).

However, some GPS-based multilayer ionosphere modeling techniques, such as computerized ionosphere tomography (CIT) and GPS radio occultation (Austen 1988, Haji et al. 1994), may improve ionosphere TEC modeling efficiency, especially in terms of horizontal accuracy and vertical resolution (Hernandez-pajares et al. 2000). Nevertheless,

Y. Yuan (✉) · J. Ou
Institute of Geodesy and Geophysics,
Chinese Academy of Sciences,
340 Xudong Road, Wuhan 430077, China
e-mail: yybgps@asch.whigg.ac.cn

Y. Yuan · C. C. Tscherning
Department of Geophysics, University of Copenhagen,
Juliane Maries Vej 30, 2100 Copenhagen Ø, Denmark
e-mail: cct@gfy.ku.dk

P. Knudsen
Department of geodesy, Danish National Space Center,
Juliane Maries Vej 30, 2100 Copenhagen Ø, Denmark
e-mail: pk@spacecenter.dk

G. Xu
GeoForschungsZentrum (GFZ) Potsdam,
Telegrafenberg A17, 14473 Potsdam, Germany
e-mail: xu@gfz-potsdam.de

single-layer ionosphere TEC modeling is still useful. This includes modeling high-accuracy local ionosphere TEC for single-station-based or network real-time kinematic (RTK) positioning and extracting precise ionospheric TEC for wide-area augmentation system (WAAS) GPS reference stations in real-time or prediction mode, in some cases (e.g., El-Arini et al. 1995; Skone 1998; Fotopoulous and Cannon 2001; Rizos and Han 2003; Zhang and Roberts 2003).

Based on the assumption of a slim ionospheric spherical shell at altitude H_{ipp} , GPS ionosphere carrier-phase (or code pseudorange)-based high-precision local (or regional or global) ionospheric TEC/delays modeling for static (or kinematic) dm (or cm or mm)-level absolute (or relative) positioning, have been achieved (e.g., Klobuchar 1987; Georgiadou and Klersberg 1988; Georgiadou 1994; Sardon et al. 1994; Qiu et al. 1995; Wang et al. 1996; Ou 1996; Komjathy 1997; Mannucci et al. 1998; Gao and Li 1998; Jakowski et al. 1999; Skone and Cannon 1999; Wilson et al. 1999; Dodson et al. 2001; Yang et al. 2001; Yuan and Ou 2001, 2002; Hernandez 2003, Skone et al. 2003; Wyllie and Zhang 2003).

However, some other factors need to be considered to further improve the work, especially to increase fitting accuracy of GPS-based ionospheric vertical TEC (VTEC) (or its corresponding frequency-dependent vertical ionospheric delay). In this regard, for a certain ionospheric region, the variation of daytime TEC is very different from nighttime TEC due to many factors, especially invisible solar radiation. Thus, the mathematical expressions of the corresponding TEC should also be different in theory. Therefore, when precisely modeling ionospheric delay using GPS data, a critical factor is to distinguish efficiently between ionospheric daytime and nighttime during different seasons over a year at the IPP, and then to select proper mathematical functions to represent the characteristics of different TEC variations associated with different periods.

In GPS, the local time t (corresponding to the longitude) and latitude of the IPP, as two important variables, are applied to construct some frequently used models (e.g., Klobuchar, spherical harmonic, polynomial and trigonometric series function models) to act as the mathematical expressions for modeling the ionosphere VTEC, directly or indirectly (Ou 1996). Since both daytime and nighttime lengths are related to seasonal and annual variations of the ionosphere, it is difficult to use only the local time to exactly distinguish between daytime and nighttime of the ionosphere, as well as efficiently represent the corresponding variations of season at a location of interest.

It is also difficult to describe precisely the variations of the ionosphere for different time periods over different seasons of a year through only a single parameterized ionosphere model. All these bring some limitations to the ionosphere TEC determination accuracy. Therefore, a possible approach to further

improve the estimation precision of GPS-based ionosphere VTEC or vertical delay may be achieved through: (1) reasonably representing both daytime and nighttime periods for the ionosphere at the IPP; (2) efficiently selecting a mathematical expression for different TEC variations; (3) investigating a new method for modeling the ionosphere effects on GPS users by combining these two improvements.

This paper introduces the concept of the ionospheric eclipse factor (IEF) λ for the IPP for relatively precise separation of daytime from nighttime for the ionosphere, and the IEF's ionospheric influence factor (IFF) $\bar{\lambda}$ for a more-efficient representation of the IEF's variations of day, month, season and year, associated with the seasonally varying TEC of the ionosphere (Yuan and Ou 2004). By combining λ and $\bar{\lambda}$ with the local time t of the IPP, a new method for modeling ionospheric delay with GPS data, called the ionospheric eclipse factor method (IEFM) is investigated. Experimental results will be used to show that the IEFM can potentially improve correction effectiveness of the ionospheric delays for GPS users over mid-latitude areas.

This paper is organized as follows: basic GPS ionospheric observation equations and principles of fitting ionospheric vertical delay or TEC with GPS data are briefly introduced in Sect. 2; the IEF is defined and a simplified determination method is illustrated in Sect. 3; Sect. 4 presents the IEFM and proposes one of its realizations for the year 2000. In Sect. 5, the validation of the correction effectiveness of the ionospheric delay fitted by the IEFM with a set of observed GPS data is given. Finally, conclusions and suggestions for future work are given in Sect. 6.

2 GPS observation equation and ionospheric delay fitting principle

It is well known that, based on zero-difference dual-frequency GPS carrier-phase measurements (ϕ_i ($i = 1, 2$)), one can obtain the geometry-free linear combination L_ϕ (Georgiadou 1994; Yuan and Ou 1999)

$$\begin{aligned} L_\phi &= F(\phi_1 - \phi_2) = I_1 + D + \varepsilon_\phi = mf \cdot I_{1,v} + D + \varepsilon_\phi \\ &= mf \cdot C_1 \cdot f_{VTEC} + D + \varepsilon_\phi \end{aligned} \quad (1)$$

where mf is the ionospheric mapping function (e.g., Ou 1996), f_i ($i = 1, 2$) is the frequency of the carrier L_i ; $F = f_2^2 / (f_1^2 - f_2^2)$; $C_i = 40.3 / f_i^2$; $I_1(I_{1,v})$ is the slant (vertical) ionospheric delays on frequency f_1 ; f_{VTEC} is the vertical TEC corresponding to $I_{1,v}$ ($= C_i \cdot f_{VTEC}$); $D = F [(N_1 - N_2) + (S_{\phi_1} - S_{\phi_2}) + (R_{\phi_1} - R_{\phi_2})]$; S and R are the instrumental biases of satellite and receiver in GPS carrier-phase data respectively; N_i is the unknown real ambiguity of L_i carrier-phase observation; ε is the combined term of observation noise and other random errors on corresponding

measurements. All quantities in Eq. (1) are expressed in units of length except the two terms F and mf .

According to Eq. (1), the vertical ionospheric delay $I_{1,v}$ (or the corresponding f_{VTEC}) may be least-square fitted along with the combined term D , which consists of both the instrumental bias and the ambiguities, using a period of observations. In this process, D is usually assumed constant for a given pair of satellite and receiver during each pass, if no cycle slips occur. A simple trigonometric function may be used as mf , which is available for GPS data with an appropriate elevation cut-off angle of greater than 25° .

Thus, from Eq. (1), one can see that the key to precise estimation of the $I_{1,v}$ (or f_{VTEC}) using GPS data is to select sound mathematical functions for properly modeling the variations of the ionosphere vertical delays (or VTEC). A new method for modeling the ionosphere vertical delays (or VTEC) will be investigated in the next two sections.

3 The ionospheric eclipse factor (IEF)

The IPP eclipse factor λ is defined as:

$$\lambda = S_{es,ipp} / S_{s,ipp} \tag{2}$$

where $S_{es,ipp}$ is the solar eclipse area seen at the IPP and $S_{s,ipp}$ is the solar apparent area seen at the IPP. The concepts of the solar eclipse area and the apparent area for a satellite can be found in Liu et al. (1997).

The variation of the time span of daytime and nighttime of the ionosphere at a certain place is mostly controlled by invisible solar radiation (e.g., Xiong et al. 1999). Both the visible and invisible solar radiation have synchronous characteristics. That is, a specific position that is in the area of visible solar radiation is usually also in the area of invisible solar radiation. There is only a small synchronous bias of the order of a few minutes between the invisible and visible radiation time periods. Such a bias only exists in the transition period between the radiation region and the shadow region for a certain location.

Thus, although λ is usually used to describe the eclipse degree of visible sunlight, it may also be considered as an approximation of the eclipse factor of invisible solar radiation experienced at the IPP. For this reason, this paper uses the eclipse factor λ of the IPP to distinguish, with a relatively precise approximation (about several minutes), daytime and nighttime of the ionosphere at the corresponding IPP. Because of this, the IPP eclipse factor λ is referred to as the ionospheric eclipse factor (IEF).

According to the IPP's IEF λ , the relation of invisible solar radiation to daytime and nighttime of the ionosphere for a fixed IPP can be preliminarily constructed as follows: when $\lambda = 0$, the IPP lies in daytime and appears in both visible and invisible solar radiations; when $\lambda = 1$, the IPP

lies in nighttime and experiences neither visible nor invisible solar radiation; when $0 < \lambda < 1$, the IPP is in the transition period between daytime and nighttime (this case will not be discussed in this paper).

One can see that the physical meaning of λ is to make a distinction between daytime and nighttime of the ionosphere at a certain point. Thus, it is feasible to describe the appearance of invisible solar radiation by improving the representation method of the appearance of visible solar radiation. If the flattening of the Earth, the Sun and some other relevant factors are not considered, a simple shadow model may be established (Liu et al. 1997). Based on this model, different values of λ can be calculated for the above corresponding eclipse factors seen at a fixed IPP.

The relative positions between the Sun, the Earth, a GPS satellite, the IPP and the reference station (receiver) are shown in Fig. 1. The vectors X_{ipp} , X_s , X^s and X_r are the positions of the IPP, the Sun, the GPS satellite, and the reference station in a same coordinate system (the Earth-fixed system is used here), respectively; z_r and z_{ipp} are the zenith angles of the GPS satellite relative to the reference station and the IPP, respectively; R_e is the mean radius of the Earth. Since $\|X_{ipp}\| = R_e + H_{ipp}$, X_{ipp} can be determined according to Fig. 1 as follows

$$X_{ipp} = X_r + \frac{\sqrt{\|X_{ipp}\|^2 + \|X_r\|^2 - 2\|X_{ipp}\|\|X_r\|\cos(z_r - z_{ipp})} \cdot (X^s - X_r)}{\|X^s - X_r\|} \tag{3}$$

$$T_\lambda = \|X_{ipp}\| \cdot \sqrt{1 - \left[\frac{\langle X_{ipp}, X_s \rangle}{\|X_{ipp}\| \cdot \|X_s\|} \right]^2} \tag{4}$$

where $\langle \cdot \rangle$ is the inner product operator and $\| \cdot \|$ is the modulus operator.

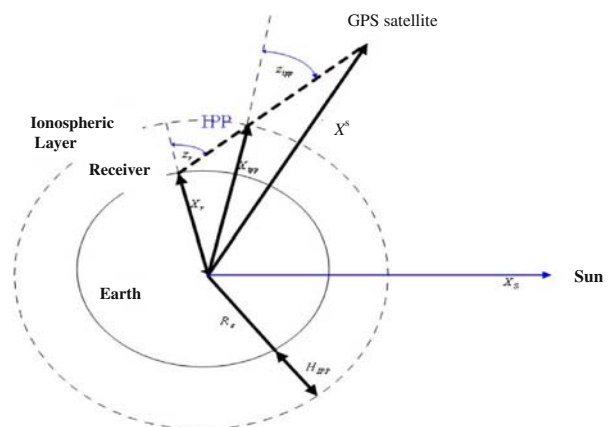


Fig. 1 Geometric relations between the Sun, the Earth, a GPS satellite, the IPP and a receiver

This paper only discusses a simple calculation of λ , which is given as follows: if $\langle X_{\text{ipp}}, X_s \rangle < 0$ and $T_\lambda < R_e$, then the IPP is in nighttime and $S_{\text{es,ipp}} = S_{s,\text{ipp}}$; otherwise, the IPP is considered to be in daytime, i.e., $S_{\text{es,ipp}} = 0$. Thus, the λ value can be written as

$$\lambda = \begin{cases} 1 & \langle X_{\text{ipp}}, X_s \rangle < 0, T_\lambda < R_e \\ 0 & \text{otherwise} \end{cases} \quad (5)$$

This calculation procedure for the IEF λ can be easily implemented in GPS software. Usually, for a given spatial position, the IEF can be computed as follows: the position vector X_{ipp} of IPP is determined firstly through the longitude, latitude and height of IPP in the inertial coordinate system; then according to the ephemeris (e.g., DE200 or DE405) provided by the Jet Propulsion Laboratory (JPL), the position vector X_s of the Sun at the corresponding epoch can be determined; finally, ionospheric eclipse factor of IPP at every epoch can be obtained using Eq. (5).

4 The IEFM for determining the ionospheric delay using GPS data

4.1 The ionospheric eclipse factor method (IEFM)

From the fundamental concept and the calculation method of the IEF λ , it can be shown that the IEF λ is more effective than the local time t in separating daytime and nighttime of the ionosphere for a fixed IPP, while the local time t is relatively more advantageous for constructing a VTEC model, especially for daytime TEC. In view of these characteristics, a new method [referred to as the IEF method (IEFM)] for modeling ionospheric delay using GPS data is proposed as follows:

- (a) Select a function f_s as the daytime VTEC model when $\lambda = 0$

Since the variation of the VTEC with respect to the local time t is relatively obvious during the daytime interval of the ionosphere over a fixed IPP, a reduced cosine function f_s , which is more easily available for modeling the daytime VTEC, is adopted to fit the corresponding VTEC.

- (b) Select a function $f_{\bar{s}}$ as the nighttime VTEC model when $\lambda = 1$

Since the VTEC does not obviously vary with the local time t during the ionospheric nighttime period at a fixed IPP, a low-order polynomial $f_{\bar{s}}$, which may usually meet the accuracy requirement for modeling the nighttime VTEC, is used to fit the corresponding VTEC. Details of the functions f_s and $f_{\bar{s}}$ will be given later in this section.

Combining (a) and (b), the IEFM can be written as

$$f_{\text{VTEC}} = (1 - \lambda)f_s + \lambda f_{\bar{s}} \quad (6)$$

Assume that, for one instant in ionospheric daytime at a fixed IPP, $f_s = f_{\bar{s}} + \widehat{f}_s$, where \widehat{f}_s is a VTEC component caused mainly by the solar effects. For simplicity, we first discuss another definition: an ionospheric influence factor (IFF) $\bar{\lambda}$ of the IEF λ . Since the IPP variation of the zenith position is similar to those IPPs nearby for a given elevation angle (above a certain mask angle), the variations and values of IEFs of IPPs in a local area are similar. Therefore, for a GPS session (a 24-hour session length is usually used for a long period of GPS data analysis; likewise in this paper), an IFF $\bar{\lambda}$ of the IEF λ is defined as

$$\bar{\lambda} = \frac{1}{n_{\text{ipp}}} \sum_{j=1}^{n_{\text{ipp}}} \lambda_{\text{ipp}_j} \quad (7)$$

where n_{ipp} is the total number of IPPs in the session, ipp_j is the j th IPP, and λ_{ipp_j} is the j th IPP's IEF. (Note that λ_{ipp_j} reflects the variations of IEF of the zenith position and its adjacent area at the j th epoch.)

Equation (7) illustrates that the values of $\bar{\lambda}$ reflect the lengths of intervals between daytime and nighttime of IPPs in different positions and different seasons. In terms of the concept of the IFF $\bar{\lambda}$ of the IEF λ , one can separate the $\bar{\lambda}$ corresponding to a long period into different intervals $[\bar{\lambda}_i, \bar{\lambda}_{i+1}]$ ($i = 1, \dots, n_{\bar{\lambda}}$, $n_{\bar{\lambda}}$ is the number of the intervals) according to the size of values of $\bar{\lambda}$.

Thus, the different intervals $[\bar{\lambda}_i, \bar{\lambda}_{i+1}]$ may represent different time periods (such as seasons or months) of the corresponding year, based on the characteristics of the variations of $\bar{\lambda}$. That is, the variation of $\bar{\lambda}$ has a seasonal property for a certain geographic position. This results in the possibility of selecting different mathematical expressions (f_s , $f_{\bar{s}}$ and \widehat{f}_s) for modeling the ionospheric VTEC corresponding to different seasons or months described by using different intervals $[\bar{\lambda}_i, \bar{\lambda}_{i+1}]$ of the IEF's IFF $\bar{\lambda}$ as follows:

$$f_{\text{VTEC},i} = (1 - \lambda)f_{s,i} + \lambda f_{\bar{s},i} \quad (8)$$

where functions $f_{\text{VTEC},i}$, $f_{s,i}$ and $f_{\bar{s},i}$ are the mathematical representations of the VTEC corresponding to the i th ionospheric time interval $[\bar{\lambda}_i, \bar{\lambda}_{i+1}]$ of a year, respectively.

4.2 An implementation of the IEFM in modeling VTEC with GPS data

In this paper, the values of $n_{\bar{\lambda}}$, $\bar{\lambda}_1$, $\bar{\lambda}_2$, and $\bar{\lambda}_3$ for the year 2000 were selected as 2, 0, 0.425, and $\max\{\bar{\lambda}_i\}_{i=1}^{n_{\bar{\lambda}}}$, where $\bar{\lambda}_3$ is the maximum value of $\bar{\lambda}_i$, respectively. According to the IEF λ and the selected intervals $[\bar{\lambda}_i, \bar{\lambda}_{i+1}]$, the selection of $f_{\bar{s}}$ and \widehat{f}_s is considered as follows:

When $\bar{\lambda}_1 \leq \bar{\lambda} < \bar{\lambda}_2$ ($[\bar{\lambda}_1, \bar{\lambda}_2]$)

$$f_{\bar{s},1} = \sum_{i=0}^{n_1} \sum_{j=0}^{m_1} a_{(i+j)} (db)^i (ds)^j, \tag{9a}$$

$$\hat{f}_{s,1} = \sum_{k=1}^{n_{k1}} a_{(n_1+m_1+k)} \cos(k \cdot h) \tag{9b}$$

When $\bar{\lambda}_2 \leq \bar{\lambda} < \bar{\lambda}_3$ ($[\bar{\lambda}_2, \bar{\lambda}_3]$)

$$f_{\bar{s},2} = \sum_{i=0}^{n_2} \sum_{j=0}^{m_2} a_{(i+j)} (db)^i (h)^j, \tag{10a}$$

$$\hat{f}_{s,2} = \sum_{k=1}^{n_{k2}} (a_{(n_2+m_2+2k-1)} \cos(k \cdot h) + a_{(n_2+m_2+2k)} \sin(k \cdot h)) \tag{10b}$$

where the a are the unknown model coefficients, $h = (t - 14)\pi/12$, t is the local time of the IPP, db is the difference between the latitude of IPP and the selected reference latitude, ds is the difference between the Sun-fixed longitude of IPP and the selected reference Sun-fixed longitude, and n and m are the total number of model coefficients. Using GPS data, the ionospheric model coefficients a_{ij} can be estimated. At the moment, the selection of the values of $n_{\bar{\lambda}_i}$, $\bar{\lambda}_i$, n_i , m_i and n_{ki} depends mainly on experience.

From Eqs. (9a) and (9b), it can be found that, thanks to the introduction of IEF and IFF, the IEFM method can relatively efficiently select and combine different mathematical expressions, such as both the polynomial and the trigonometric series function models adopted herein, for modeling different variations of the ionospheric VTEC associated with different time periods over a year. This is the dominant difference of the IEFM from other methods in which a single parameterized VTEC model (Ou 1996) is usually used and fixed during the whole period. The effectiveness of the IEFM-based fitted ionospheric delays will be validated in the following section.

5 Results and discussion

5.1 Experimental data

Dual-frequency GPS data from the IGS station WTZR (Wetzlar, Germany), with known precise coordinates, was used to conduct an experiment for analyzing the effectiveness of using the IEFM to correct the ionospheric delays from GPS data. Choosing 1 day per week over the year 2000, experiments were performed on the following days: 2, 9, 15, 22, 29, 36, 43, 50, 57, 64, 71, 78, 85, 92, 99, 106, 113, 120, 127, 134, 141, 148, 155, 162, 169, 176, 183, 190, 197, 204, 211, 218, 225, 232, 239, 246, 253, 260, 267, 273, 280, 287, 294, 301, 308, 315, 322, 329, 336, 343, 350, 357, 364.

The above GPS data was used for this test because it was in the time period of the maximum solar activity condition over the last 11-year solar cycle. A one-day session length was adopted (i.e., one day is one GPS session in this experiment). The data interval was 30 s. The elevation cut-off angle was 25° (this was to avoid using the observations with multiple paths). The selected ionospheric slim layer's height H_{ipp} was 350 km, and the adopted Earth's radius R_e was 6371.3951 km.

5.2 Experimental method

First, we use different methods and models, including the IEFM, an empirical model and the polynomial model (Ou 1996), to fit ionospheric delays for the selected time periods. Then, the fitted ionospheric delays are used to correct the corresponding single-frequency GPS P1/CA code data. Thus, the following three types of corrected P1/CA code observations can be obtained:

- Lp13 – the corrected P1/CA code observations with the ionospheric delays fitted by the IEFM;
- Lp10 – the corrected P1/CA code data with the ionospheric delays obtained from the empirical model;
- Lp11 – the corrected P1/CA code data with the ionospheric delays estimated by the polynomial model.

In addition, two other types of GPS observations were also adopted:

- Lp3 – the dual-frequency ionosphere-free linear combination of code pseudorange data (i.e. the P3 observation);
- Lp1 – P1/CA code data without correcting for ionospheric effects.

To investigate the IEFM's ability to model the ionospheric delays, the above five kinds of observations and the selected GPS data were used to conduct standard single-point positioning, and the resulting five different positioning accuracies compared. In this positioning process, except the ionosphere delay, all errors are corrected with the same methods or models as follows: satellite clock and orbital errors were reduced by using the corresponding IGS products, troposphere delays were corrected with the Saastamoinen model, and multipath effects were avoided by selection of observations tracked at elevation angles above 25°.

Hence, the differences of the absolute positioning accuracies depend mainly on the different effectiveness of the corresponding ionospheric delay corrections. This process was devised only to account for the IEFM's performance in fitting the ionospheric delays using GPS data. In this experiment,

for the IEFM, the values of n_1 , n_2 , m_1 , m_2n_{k1} and n_{k2} were selected to be 2, 1, 2, 1, 3, 6, respectively

5.3 Results and analyses

As an example to illustrate the IEFM's ability to describe different ionospheric nighttime periods with respect to different days in different seasons and months over a year, Fig. 2 compares different results of the nighttime period determined according to the local time and the IEFs of the two GPS days 197 (in summer) and 350 (in winter), 2000, at the WTZR station. From Fig. 2, the IPP's IEF is more efficient than the local time t in representing the daytime and nighttime of the ionosphere. The nighttime periods provided by the IEF efficiently vary with seasons and months, but those provided by the local time do not show similar characteristics [note that in many cases, the daytime is limited to the period between 8 and 20h, local time in the GPS community (Ou 1996)].

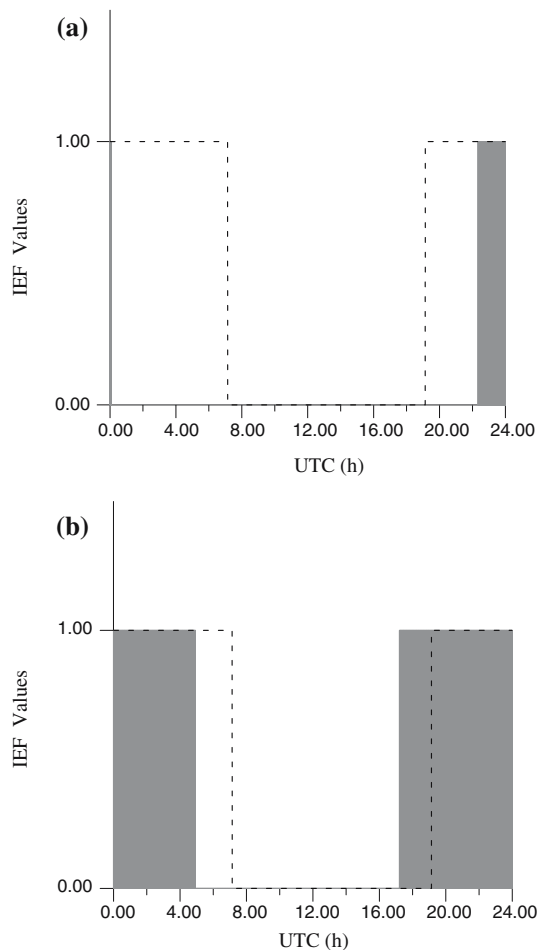


Fig. 2 A comparison of the nighttime periods determined according to the local time and the ionospheric eclipse factor (IEF) for GPS days 197 (a) and 350 (b), 2000, at the WTZR station: the dotted line denotes the nighttime period determined by the local time, the black bar denotes the nighttime period determined by the IEF

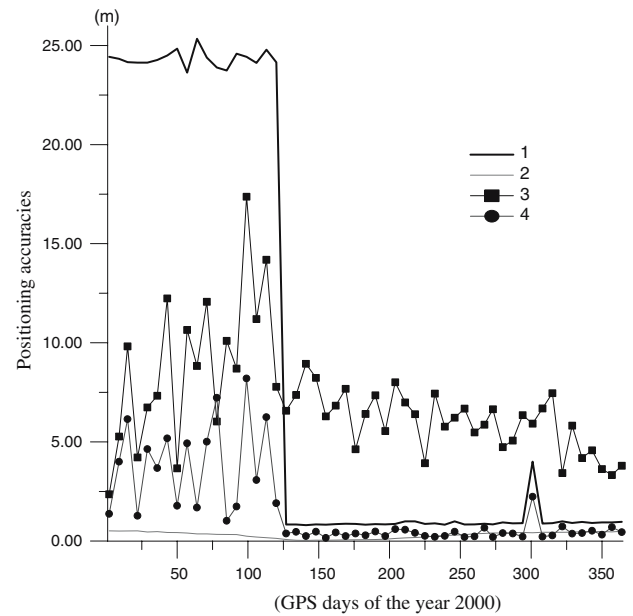


Fig. 3 Relations between the absolute positioning accuracies obtained using Lp1 and Lp3 to the IEF, 2000, at the WTZR station. 1 the RMS of unit weight of Lp3; 2 the influence factor (IFF) of the IEF; 3, 4 the absolute positioning accuracies obtained by Lp1 and Lp3, respectively

Figure 3 shows that the quality of the GPS data during the period from GPS day 2 until day 127 is obviously poorer than that of the other days due to the effects of SA. This is why the positioning accuracies for the whole year 2000 are relatively poor. In Fig. 3, the best positioning accuracy provided by the Lp3 (i.e., the ionosphere-free linear code combinations) is 0.2 m, for day 155. This is because it is the average positioning accuracy obtained by the ionosphere-free linear combination (P3) over the whole day without SA.

Furthermore, comparing the positioning accuracies obtained by Lp3 and Lp1 (i.e., the P1/CA code data without correcting the ionospheric effects), one can see that both present similar variations, due to the dominant error from SA during the corresponding period. Therefore, we separately analyzed the GPS data in the second half of 2000 when SA was off.

Figure 4 shows the positioning accuracies over the second half of 2000 (from GPS day 183 to 364) obtained using the four types of observables Lp3, Lp13, Lp11 and Lp10, as shown in lines 2, 3, 4 and 5, respectively. The annual variation of the IEF's IFF is reflected in line 1 in Fig. 4 and is also shown in line 2 in Fig. 3. The IFF's temporal variation properties show that, over the one-year time period, two similar sections can be separated according to the change of IFF, and the length of the daytime gradually becomes longer initially and then becomes shorter.

From Figs. 3 and 4, it can be seen that the positioning accuracies obtained by the Lp13 (corresponding to the IEFM) and

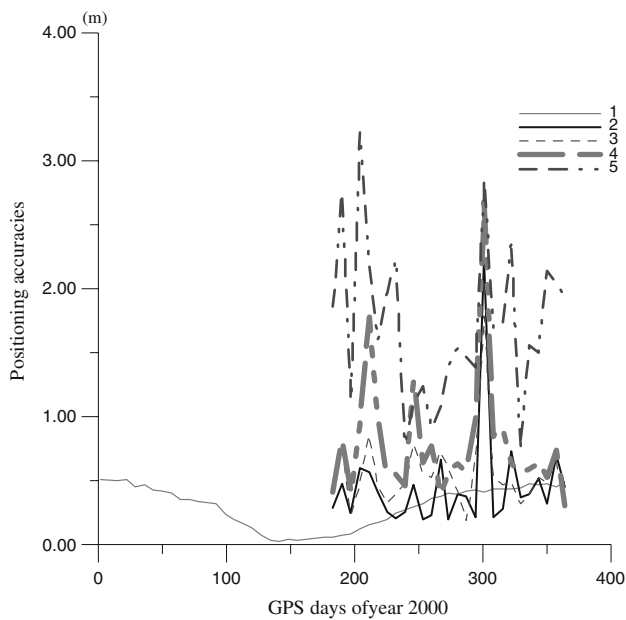


Fig. 4 A comparison of the absolute point positioning accuracies using several different methods over the second half of 2000 (from day 183 to 364), at the WTZR station. 1 the influence factor (IIF) of the IEF; 2, 3, 4, 5 the positioning accuracies obtained by the methods Lp3, Lp13, Lp11, and Lp10, respectively

the other three observables Lp3, Lp11 and Lp10 vary with the IEF’s IFF. All these demonstrate that, from the point of view of GPS ionosphere research and applications, months and seasons associated with similar invisible solar radiation may be regarded as the same ionospheric months and seasons. This indicates why one can separate different seasonal time spans of ionospheric variations in the corresponding year according to proper IFF interval divisions, as described in Sect. 4.

Table 1 gives three types of different average positioning accuracies over the whole year, the second half year and a few months of 2000 at the WTZR station, obtained by the five kinds of observations corrected with the five different ionospheric delay correction methods. In Table 1, column 1 denotes the number of GPS weeks. The numbers 52, 26 and 17 correspond to the total of GPS weeks during the three

different time periods of the whole year (from the 2nd to the 364th GPS day), the second half (from the 183rd to the 364th GPS day) and a few months (from the 183rd to the 301st GPS day) of the year 2000, respectively, as shown in column 2. The final five columns give the different average positioning accuracies obtained by the above methods over the three different time periods.

From Fig. 4 and Table 1, the positioning accuracies obtained using the Lp13 (corresponding to the IEFM) are closer to those obtained by using the Lp3 (corresponding to the ionosphere-free linear combination). This shows that the IEFM can be expected to further improve the precision of ionosphere delay correction for single-frequency GPS users.

6 Conclusions, future work and prospects

Based on establishing the ionospheric eclipse factor (IEF) λ of the IPP and its ionospheric influence factor (IFF) $\bar{\lambda}$ and internal relations and mechanisms between IEF and a selection of ionosphere models, the IEFM is presented and applied to model the ionospheric delays with GPS data, by combining λ , $\bar{\lambda}$ and the IPP local time, t .

The IEF and its IFF are advantageous for the description of the features of both the daytime and nighttime ionospheric VTEC corresponding to different time periods of ionospheric variations. The IEFM may adjust and select appropriate mathematical functions for modeling the ionosphere VTEC through considering, as far as possible, its temporal and spatial variations (annual, seasonal, and diurnal) over different areas. Experimental results demonstrate that the IEFM improves the modeling precision of GPS-based ionospheric delays.

It should be pointed out that the IEFM may be further improved and extended in terms of both theory and applications. Future work includes the following aspects: more experiments should be conducted using GPS data over different years and geographical areas, especially for different latitudes, to explore the IEFM’s applicability beyond mid-latitude regions; improving the computation method of the IEF and IFF and developing better mathematical expres-

Table 1 A comparison of the absolute point positioning accuracies using several different methods, over the whole year (2–364), the second half year (183–364) and a few months (183–301) of 2000, at the WTZR station

Number of weeks	Time periods	Lp3 ^a (m)	Lp1 ^a (m)	Lp10 ^a (m)	Lp11 ^a (m)	Lp13 ^a (m)
52	2–364	2.61	7.50	3.73	2.86	2.74
26	183–364	0.60	5.85	1.83	0.92	0.63
17	183–301	0.65	6.23	1.84	1.02	0.69

Lp10 – the corrected P1/CA code data with the ionospheric delays obtained from the empirical model

Lp11 – the corrected P1/CA code data with the ionospheric delays estimated by the polynomial model

Lp3 – the dual-frequency ionosphere-free linear combination code data (i.e., the P3 observation)

Lp1 – P1/CA code data without correcting the ionospheric effects

^a Lp13—the corrected P1/CA code observations with the ionospheric delays fitted by the IEFM

sions for modeling both daytime and nighttime VTEC of the ionosphere; enhancing the relations and physical mechanisms between IEF and a selection of ionosphere models.

In terms of applications, the IEFM may be efficiently used in scientific research and engineering applications related to high-accuracy modeling of ionospheric delays with GPS data, such as local ionosphere TEC modeling for network RTK and precise ionosphere TEC extraction for WAAS or wide area differential GPS (WADGPS) reference stations. In addition, IEFM is also suitable for modeling the ionosphere delays for kinematic space-borne single GPS receivers in low-Earth orbit satellites traveling in space at high speeds because of the IEF's ability to distinguish daytime and nighttime of the ionosphere precisely near an IPP.

Acknowledgments This work is supported by the National Natural Science Foundation of China 40625013 and the Danish National Science Foundation. Thanks go to Prof Will Featherstone, the Editor in Chief, Dr. Per Høeg and Dr. Georg Bergeton Larsen, at the Danish Meteorological Institute (DMI), and Dr. Gary Haardeng-Pedersen, at the Department of Geophysics, Australia, Ms. Anna O. Jensen, Ms. Mett and Mr. Abbas Khan, at the Danish National Space Center, for discussions and help.

References

- Austen JR, Franke SJ, Liu CH (1988) Ionospheric imaging using computerized tomography. *Radio Sci* 23(3):299–307
- Coster AJ, Foster JC, Erickson P (2003) Monitoring the ionosphere with GPS. *GPS World* 14(7):40–45
- Dodson AH, Moore T, Aquino MHO, Waugh S (2001) Ionospheric scintillation monitoring in Northern Europe. In: *Proceedings the ION GPS-2001*, Salt Lake City, pp 2490–2498
- El-Arini MB, Conker R, Albertson T, Reegan JK, Klobuchar JA, Doherty P (1995) Comparison of real-time ionospheric algorithms for a GPS wide-area augmentation system (WAAS). *Navigation J Inst Navigation* 41(4):393–413
- Feltens J, Schaer S (1998) IGS products for the ionosphere, IGS position paper. In: *Proceedings of the 1998 IGS analysis centers workshop*, ESOC, Darmstadt, Germany, 9–11 February, pp 225–232
- Fotopoulos G, Cannon ME (2001) An overview of multi-reference station methods for cm-level positioning. *GPS Solut* 4(3):1–10
- Gao Y, Li Z (1998) Ionosphere effects and modelling for regional area differential GPS network. In: *Proceedings the 11th international technical meeting of the satellite division of the US Institute of Navigation*, Nashville, Tennessee, pp 91–97
- Georgiadiou Y, Kleusberg (1988) On the effect of ionospheric delay on geodetic relative GPS positioning. *Manuscr Geod* 13:1–8
- Georgiadiou Y (1994) Modelling the ionosphere for an active control network of GPS station, LGR-series (7). Delft Geodetic Computing Centre, Delft
- Hajj GA, Ibanez-Meier R, Kursinski ER (1994) Imaging the ionosphere with the global positioning system. *Int J Imaging Syst Technol* 5:174–184
- Hernandez-pajares MJ, Juan M, Sanz J, Colombo OL (2000) Application of Ionospheric Tomography to Real-Time GPS carrier Phase Ambiguities Resolution, at Scales of 400–1,000 km and with high geomagnetic activity. *Geophys Res Lett* 27(13):2009–2012
- Hernandez-pajares M (2003) Performance of IGS ionosphere TEC maps, IGS IONO working group report, research group of astronomy and geomatics, Technical University of Catalonia (g/AGE/UPC), Barcelona, Spain, pp 16
- Jakowski N, Schlüter S, Heise H, Feltens J (1999) Auswirkungen der Sonnenfinsternis vom 11. August 1999 auf die Ionosphäre, *Allgemeine Vermessungs-Nachrichten (AVN)*, Wichmann Verlag 11–12:370–373
- Klobuchar JA (1987) Ionospheric time delay algorithm for single frequency GPS users. *IEEE Trans Aerospace Electron Syst* 23(3):325–331
- Komjathy A (1997) Global ionospheric total electron content mapping using the global positioning system. PhD Thesis, Technical report no. 188, Department of Geodesy and Geomatics Engineering, the University of New Brunswick
- Liu DJ, Guo JJ, Shi YM (1997) Principle and data processing of global positioning system. Press of Tongji University, Shanghai, pp 254–256
- Mannucci AJ, Wilson BD, Yuan DN, Ho CH, Lindqwister UJ, Rungem TF (1998) A global mapping technique for GPS-derived ionospheric total electron content measurements. *Radio Sci* 33:565–577
- Ou JK (1996) Atmosphere and its effects on GPS surveying. LGR-Series (14). Delft Geodetic Computing Centre, Delft
- Qiu WG, Lachapelle G, Cannon ME (1995) Ionospheric effect modeling for single frequency GPS users. *Manuscr Geod* 20:96–109
- Rizos C, Han S (2003) Reference station network based RTK systems—concepts and progress. *Wuhan Univ J Nat Sci* 8(2B):566–574
- Sardon E, Rius A, Zarraoa N (1994) Ionospheric calibration of single frequency VLBI and GPS observations using dual GPS data. *Bull Geod* 68:230–235
- Skone S (1998) Wide area ionosphere grid modeling in auroral region. PhD Thesis, UCGE Report 20123, Department of Geomatics Engineering, University of Calgary
- Skone S, Cannon ME (1999) Adapting the wide area ionospheric grid model for the auroral region. *Can Aeronaut Space J* 45(3):236–244
- Skone S, Cosker A, Hoyle V, Laurin C (2003) WAAS availability and performance at high latitudes. In: *Proceedings ION GPS/GNSS-2003*, Portland, pp 1279–1287
- Wang YJ, Wilkinson P, Caruana J, Wu J (1996) Real-time ionospheric TEC monitoring using GPS. In: *Proceedings of the 10th space engineering symposium*, Canberra, Australia, 27–29 March 1996, pp 101–111
- Wilson BD, Yinger CH, Feess WA, Shank C (1999) New and improved—the broadcast inter-frequency GPS World 10(9):57–66
- Wyllie SJ, Zhang KF (2003) A comparison of ionospheric models for precise positioning in Victoria In: *Proceedings the 6th international symposium on satellite navigation technology including mobile positioning and location services*, pp 1–18
- Xiong NL, Tang C, Li Xi (1999) An introduction to ionospheric physics, 1st edn. Wuhan University Press, Wuhan, pp 182–183
- Yang YX, He HB, Xu GC (2001) Adaptively robust filtering for kinematic geodetic positioning. *J Geod* 75(2–3):109–116
- Yuan YB, Ou KJ (1999) The effects of instrumental bias in GPS observation on determining ionospheric delays and the methods of its calibration. *Acta Geodaetca Cartogr Sin* 28(2):110–114
- Yuan YB, Ou JK (2001) An improvement on ionospheric delay correction for single frequency GPS user—the APR-I scheme. *J Geod* 75(5/6):331–336
- Yuan YB, Ou JK (2002) Differential areas for differential stations (DADS): a new method of establishing grid ionospheric model. *Chin Sci Bull* 47(12):1033–1036
- Yuan YB, Ou JK (2004) Ionospheric Eclipse Factor Method (IEFM) for determining the Ionospheric Delay Using GPS Data. *Prog Nat Sci* 14(9):800–804
- Zhang KF, Roberts C (2003) Network-based real-time kinematic positioning system: current research in Australia. In: *Proceedings of geoinformatics and surveying conference*, pp 1–12